Trends in Computational and Applied Mathematics, **24**, N. 2 (2023), 229-244
Sociedade Brasileira de Matemática Aplicada e Computacional
Online version ISSN 2676-0029
www.scielo.br/tcam
doi: 10.5540/tcam.2023.024.02.00229

Torques and Moments of Inertia Models for Horizontal Axis Hydrokinetic Turbine Driveline

M. H. C. BENTES[1], J. J. A. LOPES[2], K. A. PINHEIRO[3], S. de S. CUSTÓDIO FILHO[4*], J. R. P. VAZ[5] and A. L. A. MESQUITA[6]

Received on December 26, 2021 / Accepted on September 5, 2022

ABSTRACT. The quantification of torques and moments of inertia for horizontal axis hydrokinetic turbine driveline is important to precisely predict the dynamic behavior of the complete system. Initially, this paper presents different models used in the literature for describing torques and moments of inertia of turbine components. A dynamic model of a small hydrokinetic turbine using belt transmission is developed. The model uses the Blade Element Momentum (BEM) for determining the power coefficient of the turbine rotor. It considers the inertial effects and dissipative torques of the whole system. The results of the turbine dynamical behavior are compared with experimental data, showing good agreement. In order to numerically analyze a more efficient drivetrain, the belt transmission is replaced by a planetary gearbox in the model, and the new results are also assessed. It was found that with planetary gears, a more compact transmission can be used, reducing the inertial effects, bringing a better performance to the machine starting, shortening the transient regime time.

Keywords: hydrokinetic turbine, powertrain dynamics, dissipative torques, moment of inertia, belt transmission, planetary gear transmission.

1 INTRODUCTION

Hydrokinetic turbines harness the kinetic energy transported by the water stream, instead of the potential energy as in the case of traditional hydro turbines. The main importance of such a

*Corresponding author: Sérgio de Souza Custódio Filho – E-mail: sergio.custodio@ifpa.edu.br
[1]Institute of Technology, Federal University of Pará, Av. Augusto Corrêa, 01, 66075-110, Belém, PA, Brazil – E-mail: mhbentes@hotmail.com
[2]Institute of Technology, Federal University of Pará, Av. Augusto Corrêa, 01, 66075-110, Belém, PA, Brazil – E-mail: joaobernaz@gmail.com
[3]Institute of Technology, Federal University of Pará, Av. Augusto Corrêa, 01, 66075-110, Belém, PA, Brazil – E-mail: engkelvinpinheiro@gmail.com https://orcid.org/0000-0003-0612-9684
[4]Federal Institute of Pará, Fl 22, Qd Especial, 68505-065, Belém, PA, Brazil – E-mail: sergio.custodio@ifpa.edu.br https://orcid.org/0000-0001-9216-3007
[5]Institute of Technology, Federal University of Pará, Av. Augusto Corrêa, 01, 66075-110, Belém, PA, Brazil – E-mail: jerson@ufpa.br https://orcid.org/0000-0001-6440-4811
[6]Institute of Technology, Federal University of Pará, Av. Augusto Corrêa, 01, 66075-110, Belém, PA, Brazil – E-mail: alexmesq@ufpa.br https://orcid.org/0000-0001-5605-8381

technology is its implementation without significant damages to the environment [8, 9]. The installation of hydrokinetic turbines in regions with great hydrological potential is quite attractive, especially in urbanized locations where floods caused by dams (in the case of traditional hydro turbines) would be a serious problem.

Hydrokinetic turbines are not well consolidated commercially as wind turbines. But, the interest of the scientific and engineering communities on hydrokinetic technologies continue to grow. In the literature, several works have been done on kinetic turbines performance focusing on rotor optimization [4, 15, 22]. However, the electrical power produced by a kinetic turbine is influenced not only by the aero or fluid dynamics of the rotor, but also by the dynamics of the transmission and generator systems [7, 14]. Different transmission systems can be used, but in general, for small hydrokinetic turbines, belt transmission and planetary gear systems have been more frequently used [5, 11, 23]. Even a mixed transmission including both belt and gears has been used in twin-vertical axis hydrokinetic turbine [19].

For an efficient hydrokinetic turbine design, all dynamic aspects of the elements of the turbine (rotor, transmission, and generator) must be considered, especially its moments of inertia, driving and resistive torques. By individually analyzing the torques and moments of inertia of the turbine elements, it is possible to dynamically assess these elements. Several models of torques and moment of inertia have been developed in the literature. In Mesquita et al. [13] and Lopes et al. [11], hydrokinetic turbines are modelled through Blade Element Momentum Theory (BEMT) coupled with drive system and generator dynamic models. Therefore, the whole model (comprising torques and moment of inertia of the turbine elements) consisted of a nonlinear first order differential equation, which is solved by an interactive numerical method.

In this context, this current work shows initially several models of inertia and torques available in the literature, which can be used in the modeling of the turbine components. Hence, the dynamic turbine approach described in Lopes et al. [11] is presented, but under new operating conditions. The results of the model are compared with measurements in situ. In order to assess the behavior of the drive system, numerically, the belt transmission is replaced by a planetary gearbox and the results are compared.

2 DYNAMICAL MODEL

The horizontal axis hydrokinetic turbine system consists of a turbine rotor with mass moment of inertia J_T connected to a generator (electric load) with mass moment of inertia J_L, through a multiplication system with speed ratio r, and efficiency η, as shown in Figure 1. The shafts and the gears are infinitely rigid. Such consideration is valid since the vibration modes of the system are assumed to be in frequency range higher than the operational frequency range. Therefore, the dynamic equation governing the entire system shown in equation 2.1 is given by [13]:

$$T_T - (T_{D,total} + T_{L\to T}) = J_{total}\frac{d\omega_M}{dt} \tag{2.1}$$

where T_T is the turbine rotor torque, $T_{D,total}$, is the total dissipative torque of the system and $T_{L\to T}$ is the equivalent load torque. The total or equivalent mass moment of inertia of the system (J_{total}) is the sum of inertia of the turbine, inertia of the mechanical transmission, and the equivalent inertia of the generator. ω_M is the rotor angular speed of the turbine rotor.

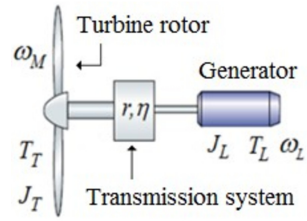

Figure 1: Illustration of the complete system of a horizontal hydrokinetic turbine [13].

The terms of torque and mass moment of inertia in equation 2.1 can be modeled in different ways. Thus, the following sections show some different models found in the literature for each term in the equation.

2.1 Turbine rotor torque

The expression of the turbine torque is obtained from the quotient between the mechanical power P_M of the rotor and its angular speed ω_M, that is:

$$T_T = \frac{P_M}{\omega_M} = \frac{1}{2}\frac{\rho\pi R^2 V^3}{\omega_M} C_P \tag{2.2}$$

where P_M is the output power of the hydrokinetic turbine, ρ is the water density, R is the radius of the turbine rotor, and V is the freestream velocity. The power coefficient C_p can be determined by the classic BEMT [6], written as:

$$C_p = \frac{8}{\lambda^2}\int_0^{\lambda} a' F(1-a)x^3 dx \tag{2.3}$$

where λ is the tip-speed ratio (TSR), x is the local-speed ratio (LSR), a and a' are axial and tangential induction factors, respectively, while F is the Prantl tip loss factor.

An empirical equation can also be used to model C_p. For the case of a turbine operating at constant or variable speed, this expression is based on experimental data provided by wind turbine manufacturers [1]:

$$C_p = c_1\left(\frac{c_2}{\lambda_i} - c_3\beta - c_4\beta^{c_5} - c_6\right)e^{\frac{-c_7}{\lambda_i}} \tag{2.4}$$

$$\lambda_i = \left(\frac{1}{\lambda + c_8\beta} - \frac{c_9}{\beta^3+1}\right)^{-1} \tag{2.5}$$

where β is the pitch angle, and c_1 to c_9 are the coefficients for approximating the curves obtained by Slootweg [21] for modern turbines.

2.2 Dissipative Torque Models

Dissipative torques are all torques resistant to the rotational movement of all elements of the turbine. For a hydrokinetic turbine, the frictional torques in bearings and the torque due to the additional mass of the fluid on the blades are considered resistive. However, for wind turbines, only the frictional torques in the bearings are considered, because the mass air is much smaller than water, which greatly reduces the drag on the rotor caused by the viscosity of the fluid. The losses of each transmission system, are accounted into their own efficiencies (η).

A simple model for the dissipative torque in the bearings is the rotating Coulomb friction model [3], which is independent of the rotation speed and given by equation 2.6:

$$T_{D,C} = \mu F_1 \frac{dm}{2} \tag{2.6}$$

where μ is the friction coefficient, F_1 is the resulting load on the bearing, and d_m is the primitive or mean diameter (between the inner and outer diameter) of the bearing. This friction torque can provide a good first estimate of the friction torque under well-controlled conditions at steady state regime.

Another simplified method to obtain the dissipative torque is described in the work developed by Bao & Ye [2], through the equation:

$$T_{D,B} = C_1 + \frac{C_2}{\omega_M} + C_3 \omega_M \tag{2.7}$$

where C_1, C_2 and C_3 are constants due to the friction of the mechanical parts imposed on the rotor.

The dissipative torque of the bearings can also be expressed depending on the type of the bearing. For example, in the case of rolling bearings, Palmgren [16] separated the dissipative torque into two types: Load-dependent component T_1 and load-independent component T_0, which is influenced by the viscous properties of the lubricant and the speed of the bearings. Therefore, the total dissipative torque for spherical bearings is obtained through the equation below:

$$T_{D,P} = T_0 + T_1 \tag{2.8}$$

where,

$$T_0 = 10^{-10} f_0 (n\nu_0)^{\frac{2}{3}} {d_m}^3 \tag{2.9}$$

$$T_1 = 10^{-3} f_1 F_\beta d_m \tag{2.10}$$

In the equations above f_0 is a factor that depends on the type of bearing and the lubrication method used, n is the speed of rotation, ν_0 is the kinematic viscosity of the lubricant, f_1 is a factor dependent on the geometry of the bearing and the relative load applied to the bearing and F_β is a factor dependent on the magnitude and direction of the applied load.

Also, for rolling bearings, SKF [20] has in its catalog another type of formulation:

$$T_{D.SKF} = T_{rr} + T_{sl} + T_{seal} + T_{drag} \tag{2.11}$$

where T_{rr} is the rolling friction torque, T_{sl} is the sliding friction torque, T_{seal} is the friction torque on the seals and T_{drag} is the frictional torque of the drag losses. Each term can be found in more detail in the SKF catalog [20].

Vaz et al. [25] used a more elaborate methodology for calculating dissipative torque. Based on SKF model [20], the Stribeck effect was considered in starting torque calculation, as shown below:

$$T_{D.SKF} = T_S e^{-\left(\frac{n}{n_{st}}\right)^i} + T_{rr} \tag{2.12}$$

$$T_S|_{n=0} = 0.5(T_{sl} - T_{seal}) \tag{2.13}$$

where n_{st} is the Stribeck speed: $n_{st} = 0.0036$; i the Stribeck exponent: $i = 1.073$ and T_{rr}, the rolling friction torque.

2.3 Generator Torque Models

The generator torque or equivalent load torque is the load torque with reference to the higher speed axis, and its expression is given by equation 2.14

$$T_{L-T} = \frac{1}{\eta} r T_L \tag{2.14}$$

where T_L is the generator torque, η is the transmission efficiency and r is the speed ratio, given by $r = \omega_L/\omega_M$.

The generator torque can be described according to the electrical parameters as shown in Vásquez et al. [24] for synchronous generator and, in Reddy & Bhagyamma [17] for asynchronous generator. However, the generator torque equation can be simplified using data from the manufacturers. Thus, a relationship between synchronous generator torque and its angular speed can be given by an approximate linear equation as shown in Bao & Ye [2]:

$$T_L = K_e \omega_L + K_0 \tag{2.15}$$

where, ω_L is the angular speed of the generator, K_e and K_0 are coefficients obtained by linear regression adjusted to the experimental data of the generator torque curve provided by the generator manufacturer.

2.4 Moment of Inertia Models

The total mass moment of inertia of the system (J_{total}) is given by the following expression:

$$J_{total} = J_T + J_f + J_{MT} + J_{L\to T} \tag{2.16}$$

where J_T is the moment of inertia of the turbine rotor mass, J_f the moment of inertia of the additive mass of the fluid around the blades (for hydrokinetic turbines), J_{MT} is the inertia of the mechanical transmission and $J_{L\to T}$ is the equivalent inertia of the generator. These moments of inertia are described as follows.

The mass moment of inertia of the J_T turbine rotor corresponds to the mass moments of inertia of the rotor blades plus the mass moment of inertia of the rotor hub. There are different mathematical models for expressing the inertia of the rotor blades. In Rosales et al. [18] the inertia of the rotor blades is given by equation 2.17

$$J_T = N\rho_b AR\left[\int (cr)^2 dr + \frac{A}{12}\left(\int c^4 \cos^2\theta_p dr + A^2 \int c^4 \sin^2\theta_p dr\right)\right] \tag{2.17}$$

where N is the number of blades, ρ_b is the fluid density, A is the blade surface area, R is the rotor radius, and c is the length of the chord as a function of r (distance increase along the length of the blade) and θ is the pitch angle of the blade.

In Mesquita et al. [13] an expression is developed to calculate the mass moment of inertia of a blade, dividing the blade into finite volumes along its profile, and at each volume, it is determined the center of mass of the volume, the mass (m_i), and the distance between the center of mass to the center of rotation of the blade (r_i). The moment of inertia of the blade root or base can be approximated as a hollow cylinder. Therefore, the equation that provides the mass moment of inertia of the blades is given by equation 2.18

$$J_{blade} = \sum_{i=1}^{N} m_i {r_i}^2 + m_{hub} {r_{hub}}^2 \tag{2.18}$$

Another way to determine the moment of mass inertia of the blades is through software dedicated to drawings and simulations, such as SolidWorks CAD 3D. In this software, it is possible to obtain the value of the moment of inertia in relation to one of the three Cartesian axes. Experimentally, the blade's moment of inertia can be obtained by measurement of frequency oscillation of the blade as a pendulum.

For wind turbines, the additive mass of the air is negligible. Therefore, the additive mass will be considered only for hydrokinetic turbines. In the literature, there are several models for the moment of inertia of the additive mass, such as Wilson [26], and Lewis & Auslaender [10] models, which were developed for marine propellers, but they can be adapted for hydrokinetic turbine rotors. More recently, Maniaci & Li [12] presented a model for the additive mass being equal to the mass of a cylinder (of length equal to the length of the blade) whose diameter is equal to the length of the chord blade.

The expression of the moment of mass inertia of the mechanical transmission can be determined from the principle that the equivalent kinetic energy of a system is equal to the sum of the kinetic energy of each component of the transmission, which is calculated according to its type of movement (translation, rotation or both). As an example, below is the moment of inertia of a one stage planetary gears transmission (Figure 2), widely used in wind and hydrokinetic turbines:

$$J_{MT} = J_{PG} = J_C + N_P\left[J_P\left(\frac{R_S + R_P}{R_P}\right)^2 + m_P(R_S + R_P)^2\right] + \left[\frac{2(R_S + R_P)}{R_S}\right]^2 J_S \tag{2.19}$$

where J_C, J_P, and J_S are the moments of inertia of the carrier, planet gear, and sun gear, respectively. N_P is the number of planet gears with radius R_P and mass m_P. R_S is the sun gear radius.

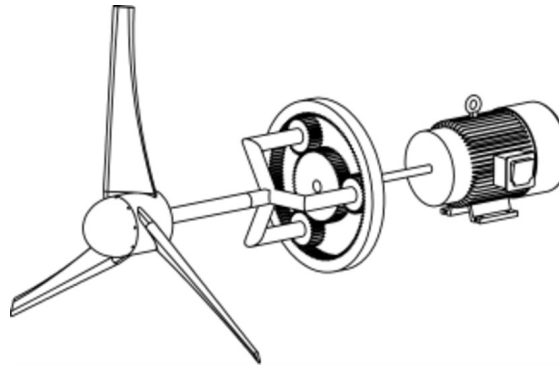

Figure 2: Illustration of a hydrokinetic turbine with planetary gear.

In the case of belt transmission (Fig. 3), applying the principle of equivalent kinetic energy, the moment of inertia of this type of transmission is given by:

$$J_{MT} = J_{BT} = J_{LP} + r^2 J_{MP} + m_B {R_{LH}}^2 \tag{2.20}$$

where J_{BT} is the moment of inertia of belt transmission, J_{LP} is the larger pulley (driver pulley), J_{MP} is the minor pulley (driven pulley), and m_B is the belt mass.

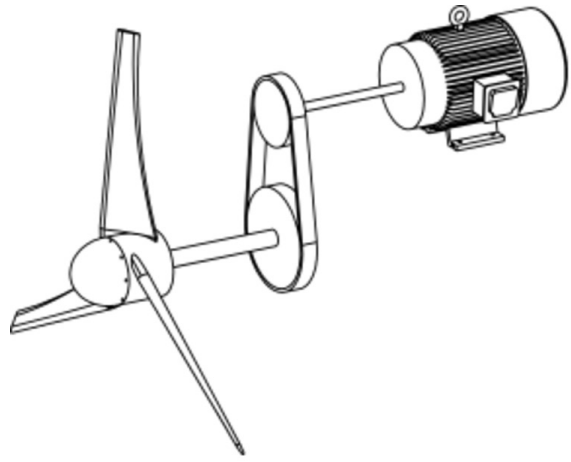

Figure 3: Illustration of a hydrokinetic turbine with belt transmission.

Regarding the moment of mass inertia of the generator, initially it is possible to use the simple model of the moment of mass inertia of a rotating cylinder, whose mass corresponds to the mass of the rotating parts of the generator. However, a correction must be made in the expression of

this inertia. In a dynamic mathematical model of the turbine with one degree of freedom, the low-speed axis is generally adopted as the reference axis, and all moments of inertia of elements on the high-speed axis must be corrected. Therefore, the moment of inertia of equivalent mass of the generator can be given by:

$$J_{L\to T} = \frac{R^2 J_L}{H} \tag{2.21}$$

where J_L is the inertia of the rotating mass of generator, which can be considered as a rotating cylinder.

As previously mentioned, there are several models of torques and moment of inertia to compose the total dynamic formulation of the turbine (equation 2.1). After completing the model, a first order non-linear ordinary differential equation is obtained, which is solved using the 4th order Runge-Kutta method. Note that, in equation 2.1, the rotor angular speed is dependent on time for any wind speed, including its fluctuations. This equation is solved considering its unsteady behavior, becoming:

$$\frac{d\omega_M}{dt} = f(t,\omega_M) = \frac{T_T - (T_{D,total} + T_{L\to T})}{J_{total}} \tag{2.22}$$

$$K_1 = f(t,\omega_M) \tag{2.23}$$

$$K_2 = f\left(t + \frac{h}{2}, \omega_M + \frac{h}{2}K_1\right) \tag{2.24}$$

$$K_3 = f\left(t + \frac{h}{2}, \omega_M + \frac{h}{2}K_2\right) \tag{2.25}$$

$$K_4 = f(t+h, \omega_M + hK_3) \tag{2.26}$$

$$\omega_M^{i+1} = \omega_M^i + \frac{h}{6}(K_1 + 2K_2 + 2K_3 + K_4) \tag{2.27}$$

where $h = t^{i+1} - t^i$ is the step-size on time. The initial value of the problem is $t^0 \approx 0$, $\omega_M^0 \approx 25$ rpm. The use od this value for ω_M^0 is due to the singularity in Eq. (2.7). The code is developed in FORTRAN90, and all the numerical solutions are performed with Intel Core i7-4720HQ computer, with 2.6 GHz processor and 16 GB RAM. Further, once the angular speed ω_M is calculated, all torque expressions dependent on time may be determined.

3 CASE STUDY

The case study refers to the measurement and numerical simulation of a small hydrokinetic turbine installed on the Arapiranga-Açu river in the city of Acará in the state of Pará, northern Brazil, located at latitude $01^o57'39$" South and longitude $48^o11'48$" West (Figure 4).

The hydrokinetic turbine is composed by a 4-bladed aluminum rotor (protected by an aluminum housing), belt transmission and a permanent magnetic generator as shown in Figure 4. The 60 cm diameter turbine rotor (illustrated in Figure 5) has four blades with 428/480 GÖ (Goetingen) profiles (480 on the blade tip and 428 on the base) combined with NACA 0012. The blade geometry is detailed in Table 1, which shows the dimensions of chord and the twist angle as a function of the radial position.

Figure 4: (a) Location of the small turbine in state of Pará, Brazil. (b) Details of the turbine installed at Arapiranga-Açu river.

Table 1: Rotor blade geometry.

Radial position [m]	Chord [m]	Twist angle [rad]
0.075	0.100	0.262
0.083	0.105	0.253
0.113	0.126	0.219
0.145	0.146	0.186
0.176	0.167	0.152
0.207	0.188	0.118
0.238	0.208	0.085
0.269	0.229	0.051
0.300	0.250	0.017

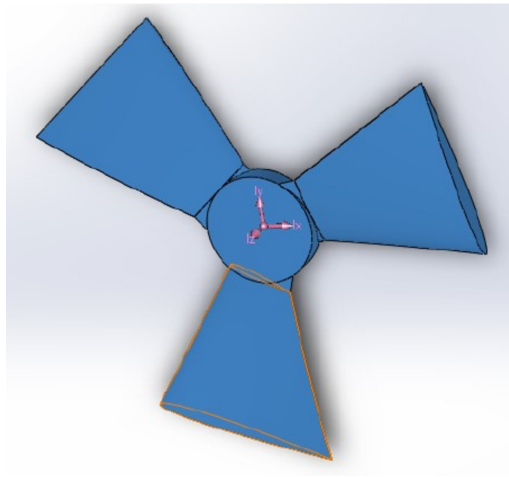

Figure 5: Illustration of 4-bladed rotor with 428/480 GÖ (Goetingen) combined with NACA 0012 profiles.

The transmission system is composed of belt and pulleys with a transmission ratio of 1 : 4. The permanent magnet generator has the following nominal characteristics: output power of 500 W, rotation of 900 rpm and output voltage of 12 V. To measure the water velocity, it was used the Sontek Flow Tracker Adv. This equipment uses the Doppler effect, and is equipped with two probes which obtain speed data in two reference axes. The rotation of the second shaft (connected to the generator) a tachometer Minipa, model MDT – 2238A was used.

The dynamical model used in the simulation is the same obtained by Lopes et al. [11] where for turbine rotor, the power coefficient is modelled by BEMT (equation 2.3). For dissipative torque from bearings, it is used Palmgren model (equations 2.8 and 2.9). The moment of inertia of blades, belt transmission and generator, equations 2.18, 2.20 and 2.21 are applied, respectively. However, for the current study, the analysis is performed for new operating conditions. In this case the river velocity has average value of 0.77 m/s, which is higher than presented in Lopes et al. [11]. Hence, the dissipative torque expression for the turbine with belt transmission is:

$$\begin{aligned} T_{D,BELT} =& 2622.899 \times 10^{-6} \omega^{0.62} + 258.12 \times 10^{-4} + 1162.788 \times 10^{-10} \omega^{0.67} \\ &+ 367.762 \times 10^{-6} \omega \end{aligned} \tag{3.1}$$

In order to assess the behavior of the drive system, numerically, the belt transmission is replaced by a planetary gearbox (see equation 2.19). The planetary transmission used in this comparison analysis has the following characteristics: transmission ratio being the same of 1 : 4, length of 0.09 m and diameter of 0.142. The transmission system has single stage with three planet gears and a sun with diameters of 0.0472 m and masses equal to 6.7749×10^{-2} kg. The carrier (Con-

nection between the rotor shaft and the planetary gears) is 0.0472 m long and mass equal to 4.6264×10^{-3} kg. In this case, the dissipative torque is given by:

$$T_{D,PLANET\ GEAR} = 249.806 \times 10^{-5}\omega^{0.67} + 453.052 \times 10^{-4} + 11.228 \times 10^{-8}\omega^{0.5} + 367.762 \times 10^{-5}\omega \tag{3.2}$$

Next, the results of rotational speed of the turbine with different models of mechanical transmissions are addressed. Further, results for turbine torque and resistive torques are presented as a function of the speed of rotation and time for both transient and steady-state behavior.

4 RESULTS

Figure 6 shows the rotational speed of the turbine with belt transmission model compared with measured data (turbine with belt transmission installed on river). In the same graph there are the results of the rotational speed when the planetary gearbox is used instead of the belt drive in the dynamical model. We observe that both mechanical transmission, planetary gearbox and belt drive, are in good agreement.

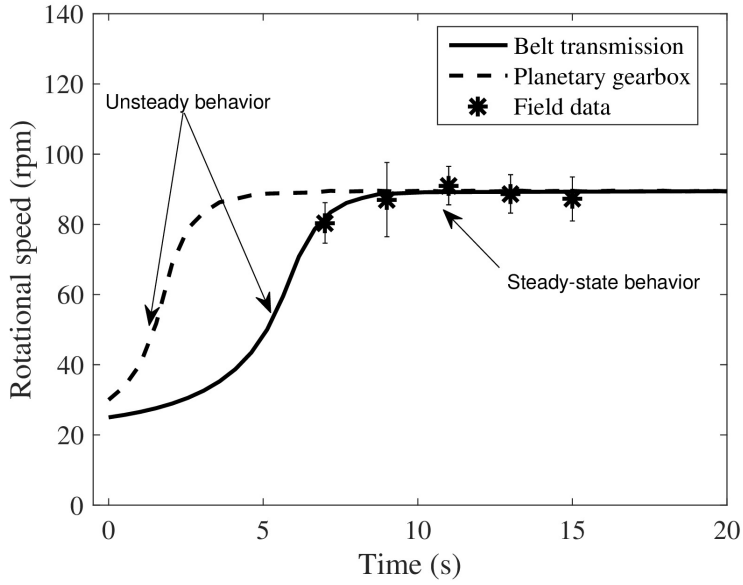

Figure 6: Results for rotational speed of the turbine for both planetary gear (numerical solution) and belt transmission (numerical and experimental data).

Note that the steady-state regime is reached more faster when the powertrain works with the planetary gearbox. This occurs because the gearbox has lower equivalent moment of inertia ($J_{PG} = 0.087 kg.m^2$) compared to the belt one ($J_{BT} = 1.76 kg.m^2$), as the resistive torques ($T_R = T_{D,total} + T_{L \to T}$) for both transmissions are quite similar (Figure 7). This implies lower

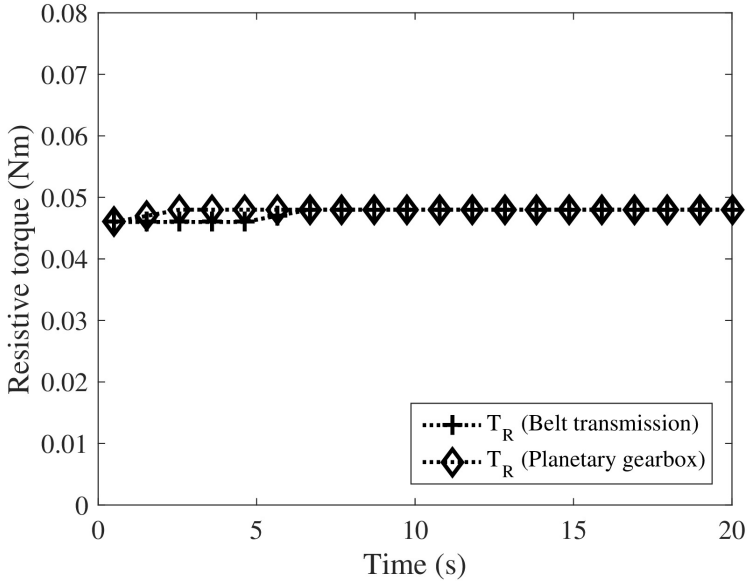

Figure 7: Results for resistive torque TR for both planetary gear and belt transmission.

energy spent by the system to reach steady-state behavior when the gearbox is used as the mechanical transmission.

The resistive torques for the turbine models with either belt transmission or planetary gears are small, as can be seen in Figure 8. The turbine torque and resistive torques are presented as a function of the speed of rotation in the transient and in the permanent regimes (where the torques match). In this way, it is noticed that a more compact transmission, with less resistance due to the lower moment of inertia brings a better efficiency in the starting of the machine. Figure 9 shows the same information as before, but with the torques shown as a function of time.

5 CONCLUSIONS

The dynamic behavior of a kinetic turbine, whether hydrokinetic or wind, can be assessed by means of the response of a non-linear dynamic model with one degree of freedom. In this dynamic model of the entire turbine, considering its driveline, there are different terms (mathematical models) described in the literature for the driving and resistive torques, as well as for the moments of inertia of the rotating components. In this sense, this paper presented a brief review of these different mathematical models available for the torque of the turbine, dissipative torque of the bearings, resistive torque of the load, and moments of inertia of the rotor, fluid, mechanical transmission, and electric generator. As a case study, the dynamic modeling of a small hydrokinetic turbine installed in the northern region of Brazil is described, which is modeled by terms

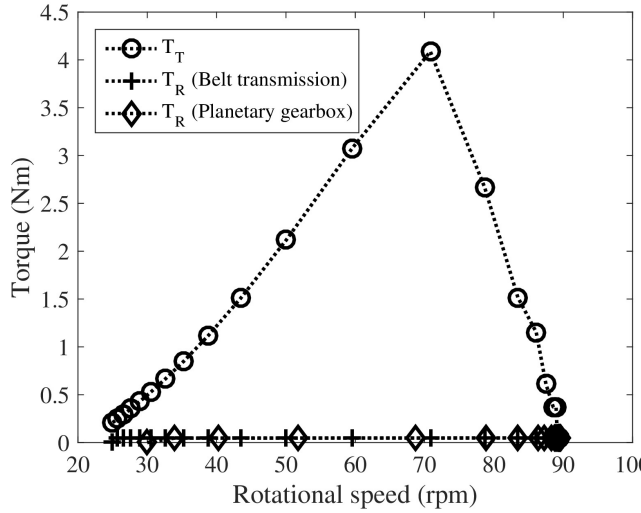

Figure 8: Results for resistive torque TR for both planetary gear and belt transmission.

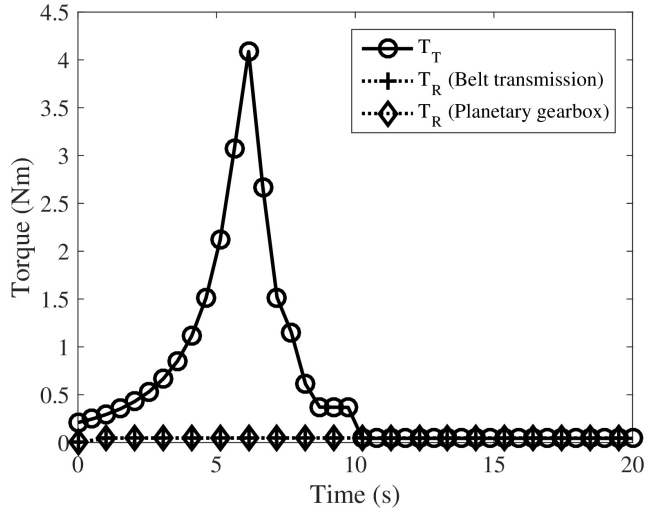

Figure 9: Comparison between the turbine torque and the resistive torque in relation to the time.

mentioned in the previous literature review. The result of the model showed excellent agreement with experimental data measured in situ.

Then, in order to assess the improvement in the efficiency of the turbine, the mechanical transmission used in the model is replaced by a transmission by planetary gears, which is a very compact transmission, with better distribution of forces, and has no slippage problems (where there is efficiency loss). The results of the new model state that the turbine, due to lower moment of inertia, has a short transient regime, therefore the steady-state regime is reached faster. This implies lower energy spent by the system to reach steady state. The turbine with the planetary gears, on the other hand, implies that the generator will be on the same center line as the turbine rotor, therefore remaining below the waterline. Therefore, the costs of manufacture, assembly, sealing are not included in this analysis.

As a limitation of the hydrokinetic system modeling by one degree of freedom is the consideration that the low and high-speed axes are considered totally rigid. This premise is valid if the operating speed range is far from the natural frequencies of the system. Otherwise, the mathematical model would have more than one degree of freedom formed by a system of non-linear differential equations, and the problem of vibrations due to resonances must be considered.

Acknowledgments

The authors would like to thank the National Academic Cooperation Program in the Amazon (PROCAD/Amazon) of the Coordination for the Improvement of Higher Education Personnel of the Brazilian Government (CAPES/Brazil), the National Council for Scientific and Technological Development (CNPq), the Amazon Foundation for Studies and Research (FAPESPA) and the Department of Research and Graduate Studies of the Federal University of Pará (PROPESP/UFPA).

REFERENCES

[1] T. Ackermann. “Wind Power in Power Systems”. Wiley (2012). URL https://books.google.com.br/books?id=y7430s86pQAC.

[2] N. Bao & Z. Ye. Active Pitch Control in Larger Scale Fixed Speed Horizontal Axis Wind Turbine Systems Part I: Linear Controller Design. *Wind Engineering*, **25**(6) (2001), 339–351. doi:10.1260/030952401760217148. URL https://doi.org/10.1260/030952401760217148.

[3] J. Brändlein, P. Eschmann, L. Hasbargen & K. Weigand. “Ball and Roller Bearings: Theory, Design and Application”. Wiley (1999). URL https://books.google.com.br/books?id=OdxSAAAAMAAJ.

[4] A. Choubey. Utilization of maximum power in airfoil blade of horizontal axis wind turbine by the concept of CFD analysis. *Journal of Urban and Environmental Engineering*, **13** (2019), 266–273. URL https://periodicos.ufpb.br/index.php/juee/article/view/44516.

[5] P. Dudhgaonkar, N. Duraisamy & P. Jalihal. Energy extraction from ocean currents using straight bladed cross-flow hydrokinetic turbine. *The International Journal of Ocean and Climate Systems*, **8**(1) (2017), 4–9. doi:10.1177/1759313116673081. URL https://doi.org/10.1177/1759313116673081.

[6] M.O.L. Hansen. "Aerodynamics of Wind Turbines: Rotors, Loads and Structure". Aktuelle Problems in der Angiologie. James & James (2000).

[7] A. Hossain, A. Iqbal, A. Rahman, M. Arifin & M. Mazian. Design and development of a 1/3 scale vertical axis wind turbine for electrical power generation. *Journal of Urban and Environmental Engineering*, **1** (2007), 53–60. URL http://www.jstor.org/stable/26203310.

[8] D. Kumar & S. Sarkar. A review on the technology, performance, design optimization, reliability, techno-economics and environmental impacts of hydrokinetic energy conversion systems. *Renewable and Sustainable Energy Reviews*, **58** (2016), 796 – 813. URL https://doi.org/10.1016/j.rser.2015.12.247.

[9] N.D. Laws & B.P. Epps. Hydrokinetic energy conversion: Technology, research, and outlook. *Renewable and Sustainable Energy Reviews*, **57** (2016), 1245 – 1259. URL https://doi.org/10.1016/j.rser.2015.12.189.

[10] F.M. Lewis & J. Auslaender. Virtual inertia of propellers. *Journal of Ship Research*, **3** (1960), 37–46.

[11] J.J.A. Lopes, J.R.P. Vaz, A.L.A. Mesquita, A.L.A. Mesquita & C.J.C. Blanco. An Approach for the Dynamic Behavior of Hydrokinetic Turbines. *Energy Procedia*, **75** (2015), 271–276. doi:https://doi.org/10.1016/j.egypro.2015.07.334. URL https://www.sciencedirect.com/science/article/pii/S1876610215011029. Clean, Efficient and Affordable Energy for a Sustainable Future: The 7th International Conference on Applied Energy (ICAE2015).

[12] D.C. Maniaci & Y. Li. Investigating the influence of the added mass effect to marine hydrokinetic horizontal-axis turbines using a General Dynamic Wake wind turbine code. In "OCEANS'11 MTS/IEEE KONA" (2011), p. 1–6. doi:10.23919/OCEANS.2011.6107276.

[13] A.L.A. Mesquita, A.L.A. Mesquita, F.C. Palheta, J.R.P. Vaz, M.V.G. de Morais & C. Gonçalves. A methodology for the transient behavior of horizontal axis hydrokinetic turbines. *Energy Conversion and Management*, **87** (2014), 1261 – 1268. URL https://doi.org/10.1016/j.enconman.2014.06.018.

[14] J.L. Moreira, A.L. Mesquita, L.F. Araujo, M.A. Galhardo, J.R. Vaz & J.T. Pinho. Experimental investigation of drivetrain resistance applied to small wind turbines. *Renewable Energy*, **153** (2020), 324–333. doi:https://doi.org/10.1016/j.renene.2020.02.014. URL https://www.sciencedirect.com/science/article/pii/S0960148120302007.

[15] A. Muratoglu, R. Tekin & Ömer Faruk Ertuğrul. Hydrodynamic optimization of high-performance blade sections for stall regulated hydrokinetic turbines using Differential Evolution Algorithm. *Ocean Engineering*, **220** (2021), 108389. doi:https://doi.org/10.1016/j.oceaneng.2020.108389. URL https://www.sciencedirect.com/science/article/pii/S0029801820312968.

[16] A. Palmgren, G. Palmgren, B. Ruley & i. SKF Industries. "Ball and Roller Bearing Engineering". SKF Industries, Incorporated (1945). URL https://books.google.com.br/books?id=sdtSAAAAMAAJ.

[17] G.P.K. Reddy & S.S.D.S. Bhagyamma. "Fixed-Speed and Variable Speed (PMSG) Induction Generators Based Wind Farms with Statcom Control under Asymmetrical Grid Faults" (2014).

[18] P. Rosales, J. Cerezo, G. Montero & A. Lambert. Comparative Assessment of a Horizontal Small Wind Turbine with Ball and Magnetic Bearings on the Starting. *Chemical Engineering Transactions*, **34** (2013), 55–60. doi:10.3303/CET1334010. URL https://www.cetjournal.it/index.php/cet/article/view/CET1334010.

[19] S. Runge, T. Stoesser, E. Morris & M. White. Technology readiness of a vertical-axis hydro-kinetic turbine. *Journal of Power and Energy Engineering*, **6** (2018), 63–85. URL https://doi.org/10.4236/jpee.2018.68004.

[20] SKF. Rolling Bearing Catalogue (2018). URL www.skf.com.

[21] J. Slootweg. "Wind Power: Modelling and Impact on Power System Dynamics". Doctoral thesis, Technical University of Delft, Delft, Netherlands (2003). URL http://resolver.tudelft.nl/uuid:f1ce3eaa-f57d-4d37-b739-b109599a7d21.

[22] N. Tenguria, N.D. Mittal & S. Ahmed. Evaluation of performance of horizontal axis wind turbine blades based on optimal rotor theory. *Journal of Urban and Environmental Engineering*, **5** (2011), 15–23. URL http://www.jstor.org/stable/26203352.

[23] W. Tian, Z. Mao & H. Ding. Design, test and numerical simulation of a low-speed horizontal axis hydrokinetic turbine. *International Journal of Naval Architecture and Ocean Engineering*, **10**(6) (2018), 782–793. doi:https://doi.org/10.1016/j.ijnaoe.2017.10.006. URL https://www.sciencedirect.com/science/article/pii/S2092678217301978.

[24] F.A.M. Vasquez, T.F. de Oliveira & A.C.P. Brasil Junior. On the electromechanical behavior of hydrokinetic turbines. *Energy Conversion and Management*, **115** (2016), 60 – 70. doi:https://doi.org/10.1016/j.enconman.2016.02.039.

[25] J.R. Vaz, D.H. Wood, D. Bhattacharjee & E.F. Lins. Drivetrain resistance and starting performance of a small wind turbine. *Renewable Energy*, **117** (2018), 509–519. doi:https://doi.org/10.1016/j.renene.2017.10.071. URL https://www.sciencedirect.com/science/article/pii/S0960148117310339.

[26] W. Wilson. "Practical Solution of Torsional Vibration Problems: With Examples from Marine, Electrical, Aeronautical, and Automobile Engineering Practice". v. 4. Chapman & Hall (1956).